PROCEEDINGS OF SPIE

SPIEDigitalLibrary.org/conference-proceedings-of-spie

SCOTS: a reverse Hartmann test with high dynamic range for Giant Magellan Telescope primary mirror segments

Peng Su
Shanshan Wang
Manal Khreishi
Yuhao Wang
Tianquan Su
Ping Zhou
Robert E. Parks
Kevin Law
Mario Rascon
Tom Zobrist
Hubert Martin
James H. Burge

SPIE.

SCOTS: A reverse Hartmann test with high dynamic range for Giant Magellan Telescope primary mirror segments

Peng Su[1*], Shanshan Wang[2], Manal Khreishi[1], Yuhao Wang[1], Tianquan Su[1], Ping Zhou[1],Robert E. Parks[1], Kevin Law[3], Mario Rascon[3], Tom Zobrist[3], Hubert Martin[3] and James H. Burge[1,3]

[1]*College of Optical Sciences, the University of Arizona, Tucson, AZ 85721, USA*
[2]*Department of Opto-electronics, Beijing Institute of Technology, Beijing, China*
[3]*Department of Astronomy/Steward Observatory, the University of Arizona, Tucson, AZ 85721, USA*
psu@email.arizona.edu

ABSTRACT

A software configurable optical test system (SCOTS) based on fringe reflection was implemented for measuring the primary mirror segments of the Giant Magellan Telescope (GMT). The system uses modulated fringe patterns on an LCD monitor as the source, and captures data with a CCD camera and calibrated imaging optics. The large dynamic range of SCOTS provides good measurement of regions with large slopes that cannot be captured reliably with interferometry. So the principal value of the SCOTS test for GMT is to provide accurate measurements that extend clear to the edge of the glass, even while the figure is in a rough state of figure, where the slopes are still high. Accurate calibration of the geometry and the mapping also enable the SCOTS test to achieve accuracy that is comparable measurement accuracy to the interferometric null test for the small- and middle- spatial scale errors in the GMT mirror.

Keyword: Optical metrology, Optical testing, Hartmann test, Fringe reflection, deflectometry

1. Introduction

The Giant Magellan Telescope (GMT) is a 25-m extremely large telescope for use at optical and infrared wavelengths [1]. The GMT primary mirror consists of seven, 8.4-m, spin-cast, borosilicate, honeycomb segments manufactured by the Steward Observatory Mirror Lab. The parent surface of the seven-segment primary mirror has a radius of curvature of 36 m and a conic constant of -0.998. The six identical off-axis segments have a P-V aspheric departure greater than 14 mm. The first 8.4-m off-axis mirror segment has been recently completed and the second segment is underway [2].

In order to achieve a high level of confidence in the required precision of testing the primary mirror segments, a suite of independent tests is required [3]. The principal optical test is a full-aperture interferometric null test. A 3.75-m large fold sphere (LSF), an additional 76 cm fold sphere and a computer-generated hologram correct the 14 mm aspheric departure of the off-axis mirror segments [4]. The principal test is mainly used once the mirror has been polished to produce a specular surface with residual slope errors of moderate amplitude. During generating and fine grinding the surface was measured using a laser tracker plus system [5]. A third redundant test of the global figure was provided by a scanning pentaprism test that simulates a plane-parallel wavefront incident on the mirror segment. The main purpose of the pentaprism test is to provide an independent measurement of low-order aberrations and segment geometry. It can also measures small-spatial scale structure, but only measures slopes in scan lines in the radial direction [6]. A different slope test, the Software Configurable Optical Test System (SCOTS), was developed to measure small- and mid-scale errors on highly aspheric surfaces [7, 8]. Applied to the

Modern Technologies in Space- and Ground-based Telescopes and Instrumentation II,
edited by Ramón Navarro, Colin R. Cunningham, Eric Prieto, Proc. of SPIE Vol. 8450, 84500W
 · doi: 10.1117/12.926719

GMT segment, the SCOTS test is complementary to the pentaprism test. Together, these tests provide independent confirmation of the principal optical test.

This paper is organized as follows. In Section 2, we outline the basic principle of SCOTS. In Section 3 we describe how SCOTS is applied to the GMT mirror and show some metrology results and discussion. Finally, conclusions and perspectives are drawn in Section 4.

2. Principle of SCOTS

SCOTS is based on the geometry of the fringe reflection/phase measuring deflection [9-11] for rapidly, robustly, and accurately measuring large, highly aspherical shapes. The detailed principles of the SCOTS are shown in [7, 8] and summarized below.

2.1 Reverse Hartmann test, triangulation, centroiding model and synchronous detection

SCOTS can be better understood referring to a traditional Hartmann test [12] with the light going through the system in reverse; see Fig. 1(a) and (b). Fig. 1(b) shows schematically how the surface slope is measured and calculated. The flat panel display is set up with its screen near the center of curvature and facing the mirror under test. If a single pixel is lit up on the otherwise dark screen, the camera's CCD detector which is focused on the mirror surface will show a bright region corresponding to the area on the mirror where the angle of incidence from the bright pixel on the screen is equal to the angle of reflection back to the camera. The angular bisector of the incident and reflected rays is normal to the surface at the bright point. The surface slopes at the bright spots can be calculated based on triangulation using the coordinates of the lit screen pixel, the camera aperture center, and the reflection of the illuminated pixel captured by the CCD. The slopes can be integrated using a polynomial fit to the slopes or by a zonal integration method to give the surface shape.

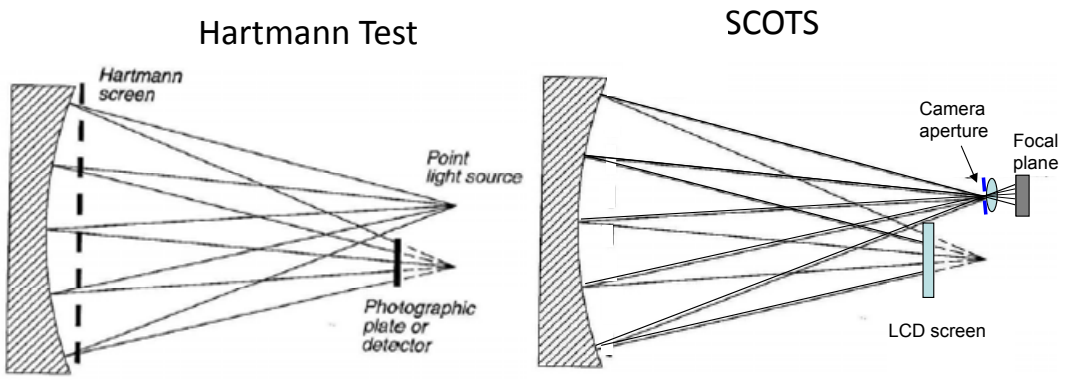

Figure 1. Comparison of the test geometry for the classical Hartmann test and for SCOTS.

In a Hartmann test, a point source of light at the center of the curvature reflects off the surface being tested. The pupil is divided into numerous sample regions with a mask, and the light from each of these regions refocuses on a detector. The positions of the refocused light spots indicate the slope of the surface in each of the regions, and these slopes can be compared with those for a theoretically perfect surface. In SCOTS, it is useful to visualize the system backward, where the rays start from the camera aperture, hit the mirror, and are reflected towards the screen. Now the screen has the function of the detector in the Hartmann test, while the camera works as the point source. Moreover, because the camera takes the images of the mirror during the test, it also supplies information about the

pupil coordinates (the positions on the mirror where the slopes are measured), which correspond to the Hartmann screen hole positions. Each illuminated camera pixel samples a certain region of the test mirror. We call this region the mirror pixel for convenience in the following discussions. With a finite size of the camera aperture, multiple screen pixels may light up the same mirror pixel. Analogous to the Hartmann test, the average slope at a mirror pixel can be measured by evaluating the centroid (first moments) of the corresponding screen pixels and then the centroid values are used for the triangulation calculation.

The centroiding process supplies sub-pixel slope measurement which provides the high slope sensitivity of the test. The reverse Hartmann geometry replaces the relatively small format detector with a large size screen that produces a much larger dynamic range in slope variation for the test. By using the camera to map the test surface this significantly increases the test surface spatial sampling density over the traditional Hartmann test.

Based on the above discussion, we need to determine the correspondence between the screen pixel location and a particular mirror pixel to do the triangulation calculation. This can be done efficiently by coding the screen pixels. A common way to do this is to code the screen pixels with an intensity variation such as displaying sinusoidal fringes on the screen. By phase shifting the fringes and taking synchronous pictures, the phase value that corresponds to a screen pixel coordinate at a certain mirror pixel can be found using quadrature detection techniques.

2.2 Transverse ray aberration model

In many cases of testing a polished spherical or aspherical optical surface or an optical system, the test surface is close to the ideal surface within a few microns. The relative positions between the test surface, the camera and the screen can be well controlled during the alignment, for instance with a distance measuring interferometer such as a laser tracker [13]. In this situation, the measurement can simply be thought of as a comparison between the ideal transverse ray aberration distribution and the measured transverse ray aberration from the screen centroiding or phase shifting calculation. The transverse ray aberration can be transformed into the system wavefront aberration using an exact equation as in (1) [14].

$$\frac{\partial W(x,y)}{\partial x} = -\frac{x_{screen}}{R - W(x,y)}, \quad \frac{\partial W(x,y)}{\partial y} = -\frac{y_{screen}}{R - W(x,y)} \tag{1}$$

Here $W(x,y)$ is the wavefront aberration (departure from spherical), x and y are exit pupil coordinates of the system, R is the radius of the reference sphere, x_{screen} and y_{screen} are the transverse ray aberrations. The slopes can then be integrated using a polynomial fit to the slopes or by a zonal integration method to give the system wavefront as well as the surface departure from the ideal shape.

3. SCOTS for GMT

3.1 Basic setup

We applied SCOTS to measure the 8.4m-diameter off-axis GMT primary mirror segment to enable measurements of the edge, where the large slopes limited the accuracy of the interferometry. The interferometric GMT test used a set of null optics that included a 3.75m tilted sphere, a 1m sphere, a computer-generated hologram, and an instantaneous phase-shifting interferometer. The interferometric null test optics, other than the 3.75m sphere, were mounted together on an optical bench. It was not possible to locate the SCOTS test hardware near the center of curvature of the GMT mirror segment, so we placed the LCD-monitor screen and the CCD camera above the optical bench and used the 3.75m tilted sphere as part of the test as shown in Fig. 2. In this configuration, the SCOTS test was non-null and used an area of approximately 220×40 mm on the screen to completely cover the mirror with fringes.

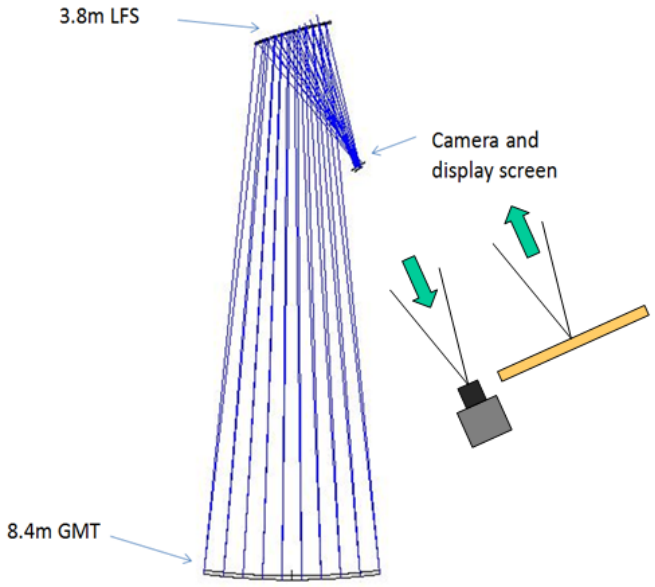

Figure 2. GMT SCOTS test setup showing the test, as folded with the 3.8-m Large Fold Sphere. The inset to the right is an enlarged view of the camera and screen.

3.2 Test model

A transverse ray aberration model was used for the GMT SCOTS test. In Eq. (1), the ray aberrations at each CCD image pixel were calculated from the screen centroiding or phase shifting to sub-pixel accuracy. However, we still need to accurately determine how the image pixels were related with exit pupil coordinates of the test system and also to the mirror surface coordinates for computer controlled polishing (CCP) of the surface errors.

As the exit pupil is the image of the test system stop which is the GMT mirror itself, it can be varied as the alignment of the LFS varies. To avoid this possibility, we measured the ray aberrations in the mirror surface coordinate system as it was easy to access to put fiducials on it for mapping calibration, and the mirror surface coordinates are directly related to the CCP fabrication map.

We basically evaluate the transverse-ray-aberration departure from the ideal and then integrate the difference to get the test mirror surface errors. A scaling factor which is similar to R in Eq. 1 for transferring ray aberrations to surface slope errors was calculated from the numerical model. Fig. 3 shows the ideal slopes for the test system, which were calculated by dividing the transverse ray aberrations by the scaling factor. Fig. 4 gives the ideal spot diagram created from the ideal transverse ray aberrations. It was not possible to locate the screen or camera at the ideal positions, which would have minimized the geometric size of the spot diagram. The SCOTS camera and screen were required to stay clear of the light path for the interferometric null test.

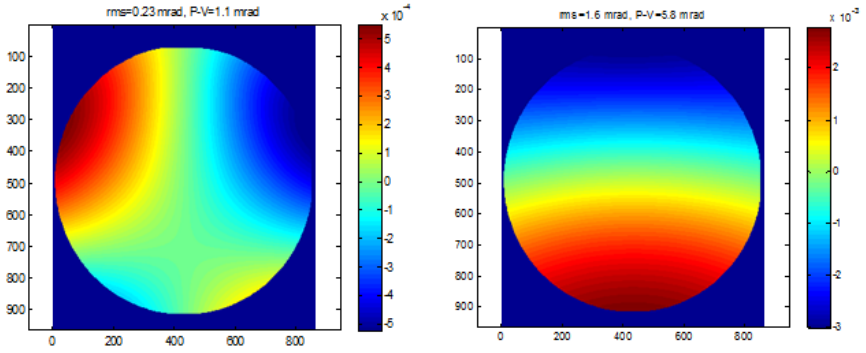

Figure 3. Ideal x and y slopes for the SCOTS non-null test of the GMT mirror segment.

Figure 4. The ideal spot diagram for the SCOTS GMT test, an area of approximately 220×40 mm on the monitor screen.

3.3 Mapping calibration

The uncertainty in the coordinates of where the slope is being measured will introduce errors that are proportional to the slope variation. As the test is non-null, this effect can be significant. Figure 5 shows the x slope error/x mapping error (mean=0.09 μrad/mm), the y slope error/y mapping error (mean=0.7 μrad/mm), and the y slope error/x mapping error, and the x slope error/y mapping error (mean=0.06 μrad/mm). These reflect the sensitivity of slope measurements to the mapping uncertainty. The dominant errors are in y direction ranging from 0.3 to 0.9 μrad slope measurement error per mm of mapping error.

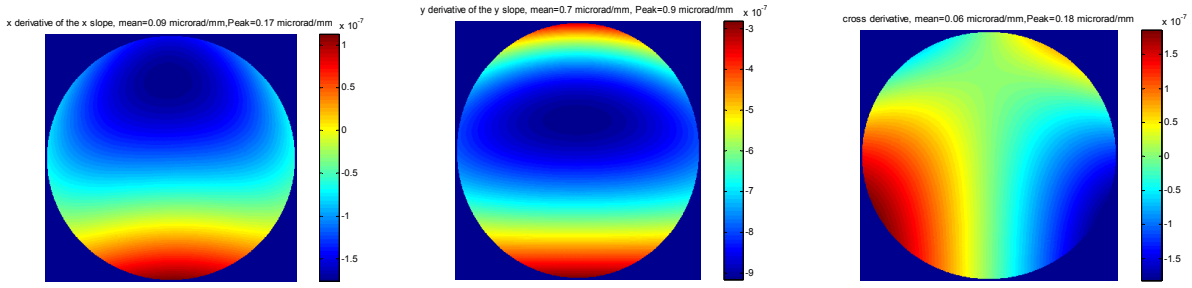

Figure 5. The sensitivity of slope measurements to the mapping uncertainty. (a) the x slope error/x mapping error (mean=0.09 μrad/mm), (b) the y slope error/y mapping error (mean=0.7 μrad/mm), (c) the y slope error/x mapping error and the x slope error/y mapping error (mean=0.06 μrad/mm).

The mapping of the mirror coordinate system is inherently nonlinear. The camera usually is not perfect and has imaging distortion, and imaging aberration. The camera and the LFS form a combined imaging system because the

camera sees the test mirror through the LFS, moreover, the mirror surface itself is in a curved shape. We calibrated the mapping of the SCOTS test by placing customized fiducial references on top the mirror as shown in Fig. 6 (a). The position of each fiducial was measured using a laser tracker, and the location of the image was determined by centroiding. The imaging distortion was then mapped back to mirror coordinates using a set of vector polynomials which are orthonormal in a unit circle [14, 15]. A mapping accuracy of less than 0.5 mm at the mirror surface was achieved.

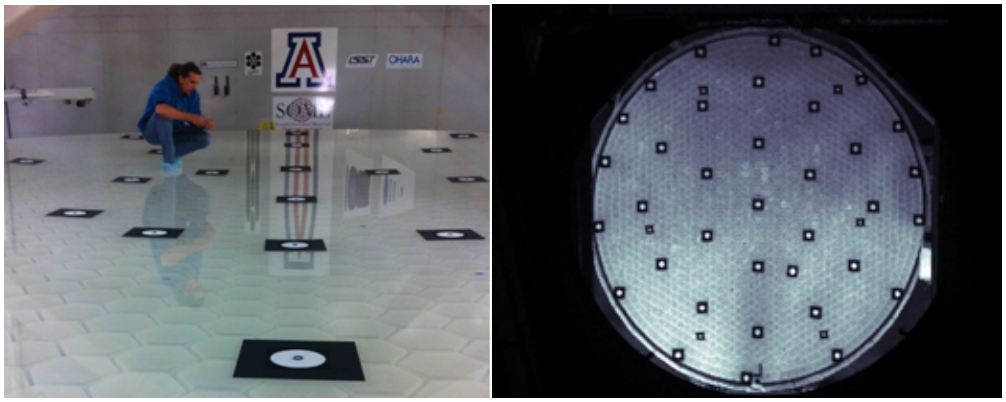

Figure 6. GMT SCOTS test mirror fiducials and the fiducial image obtained by SCOTS camera.

3.4 Data collection and test results

Sinusoidal fringes in the x and y directions were displayed on the LCD screen and the corresponding images of the GMT mirror were recorded as seen in Fig. 7. Phases which correspond to the transverse ray aberrations were calculated and unwrapped. The phase maps were then corrected for distortion. Further, ideal shape data were subtracted and the residuals were integrated to give the test surface map.

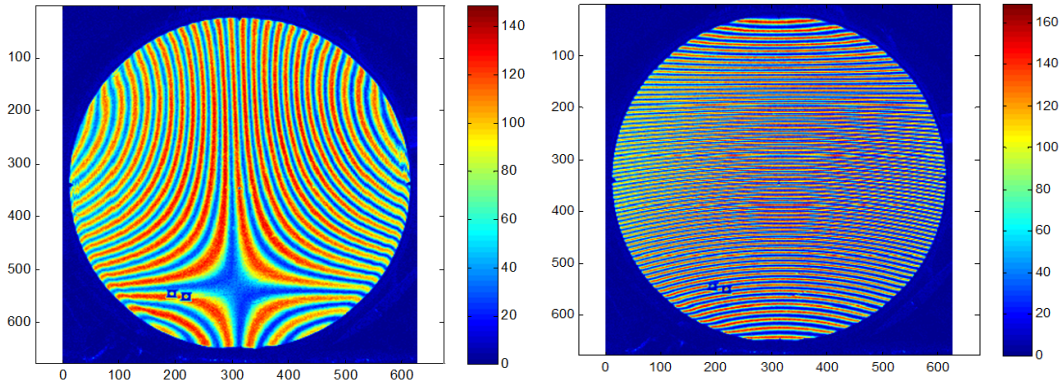

Figure 7. Fringe images of the GMT SCOTS test.

Figure 8 shows a comparison of the null interferometric test result with the SCOTS test result when the GMT mirror was at the eary stage of figuring. As we can see the interferometric test had difficulty obtaining data outside 90% of the mirror aperture because of the high slopes at the edge of the mirror. Over the central 90% of the mirror aperture, where both methods achieved good data, the SCOTS data compared well with the interferometric data (errors in the LFS were not subtracted at this time). Low order terms related to the test system alignment were removed from both maps.

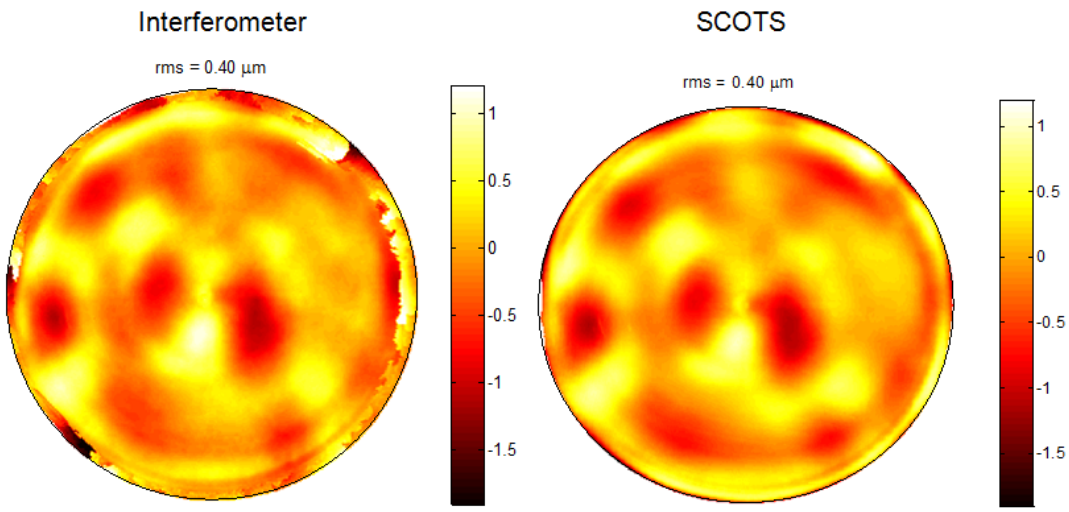

Figure 8. Early comparison of the interferometric map and SCOTS map of the GMT surface figure error. These measurements were made when the mirror was at the early stage of figuring and some slopes near the edge provided difficulty for interferometry. (Low order terms are removed from both measurements.)

The SCOTS system is capable of making very accurate measurements when the geometry is controlled and all aspects are well calibrated. A demonstration of the accuracy was made for the measurement of the 3.8-m diameter fold sphere. This mirror was measured as it is supported, face-down for the GMT test. A direct comparison between the interferometric measurment for center of curvature and the SCOTS measurement is shown below in Figure 9.

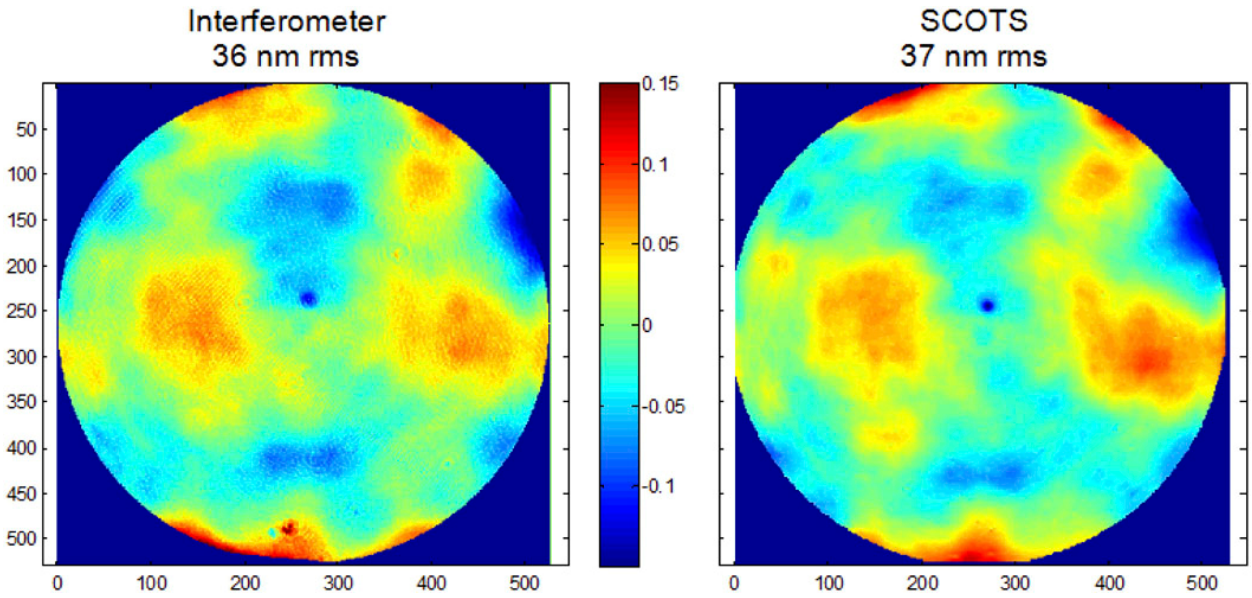

Figure 9. Comparison of the interferometric map and SCOTS map of the 3.8-m fold sphere used for GMT. This is a spherical mirror, measured by the interferometer and SCOTS directly from the center of curvature, so these measurements lack many of the systematic errors present in the measurements of the GMT segment

The measurement of the 3.8-m sphere provides a good demonstration of the inherent sensitivity of the SCOTS test. But sincethis mirror is measured directly from center of curvature, very little calibration is required to achieve high accuracy. The accuracy for the GMT measurement is limited by calibrations of systematic effects.

Figure 10 shows a comparison interferometric and SCOTS measurements that were made of the GMT at a stage late in the figuring where both tests provide good data over 95% of the surfacer. A direct subtraction of the two maps shows a difference ~25 nm rms and this is within the uncertainty level of both the interferometric test, and the SCOTS measurements.

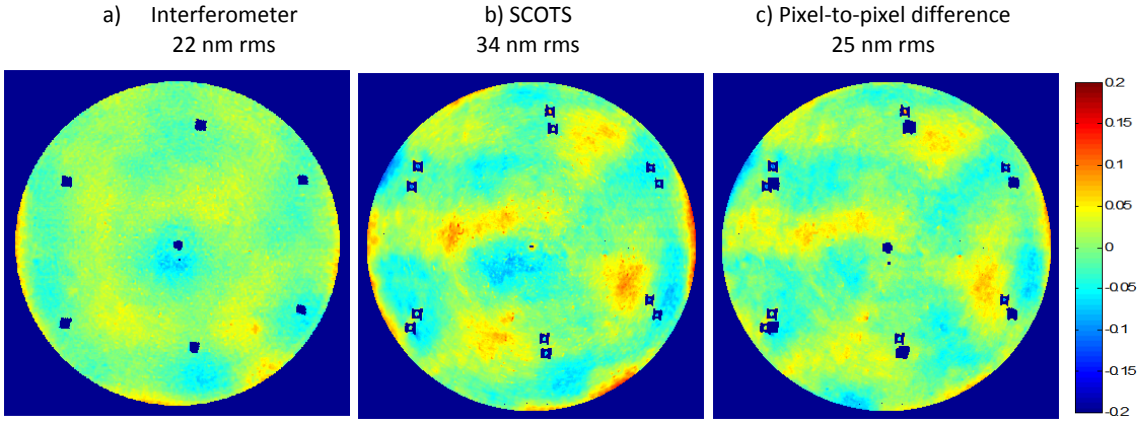

Figure 10. Comparison of the interferometric map and SCOTS map over 95% mirror diameter (low order terms removed). (a) Interferometric map rms=22 nm, (b) SCOTS map rms=34 nm, (c) direct subtraction of the two maps rms=25 nm.

In Fig 10, both the interferometric map and the SCOTS map have the errors from LFS removed. Fig. 11 shows the LFS map for SCOTS which was generated by morphing the LFS center of curvature interferometric map taking into account the fact that the SCOTS test has “retrace error”, that is the ray path to the LFS for the outgoing rays is different from the rays reflected in the GMT mirror. This is clearly shown in Fig. 10 (b) and (c) where the 6 fiducials on the LFS show up as two sets of fiducials. Fig. 11 (a) shows the two rays paths on the LFS. The maximum shift between the two reflections is ~150mm.

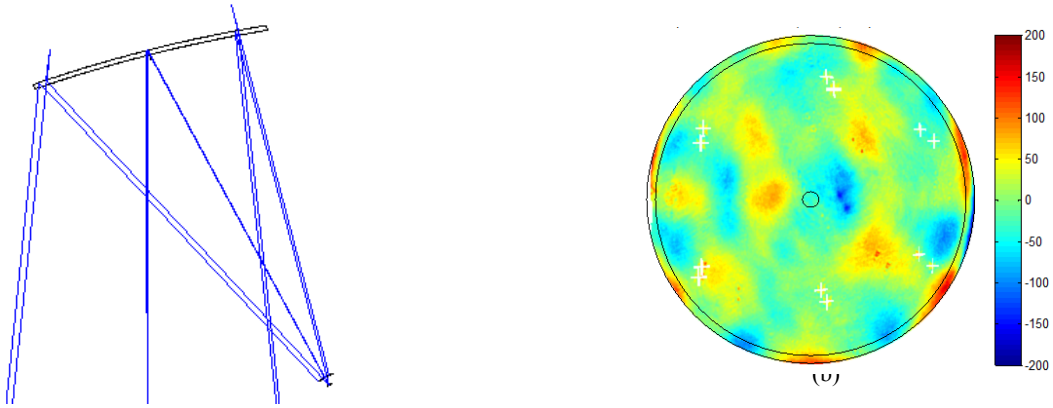

Figure 11. The SCOTS measurement of the GMT requires the light to reflect twice off the fold sphere. Unlike the interferometric test, these two reflections are not coincident (a) Ray path in the SCOTS test shows the two reflections from LFS. The maximum shift between the two is ~150mm. (b) LFS map for the GMT SCOTS test, rms=37 nm.

4. Summary

The SCOTS measurement technique provides invaluable information early in the processing where high slopes limit the ability to achieve reliable data with the interferometer. The SCOTS measurement of the GMT primary mirror segment shows good agreement with the null interferometric test. As such, SCOTS helps verify the middle spatial frequency figure errors in the test mirror. For future work, there is the potential to further increase the measurement accuracy of SCOTS for low spatial frequency components by improving the mapping calibration and the system alignment precision, and to improve the high frequency measurements with improved imaging. SCOTS, as a non-null large dynamic range and high accuracy test method, provides an invaluable metrology tool for aspheric surface fabrication.

5. References

[1] M. Johns, "The Giant Magellan Telescope (GMT)", *Ground-based and Airborne Telescopes*, Proc. SPIE **6267**, (2006).

[2] H.M. Martin, *et.al*., "Production of 8.4 m segments for the Giant Magellan Telescope," Proc. SPIE **8450** (2012).

[3] J. H. Burge, W. Davison, H. M. Martin and C. Zhao, "Development of surface metrology for the Giant Magellan Telescope primary mirror", Proc. SPIE **7018** (2008).

[4] S.C. West, J.H. Burge, B. Cuerden, W. Davison, J. Hagen, H.M. Martin, M.T. Tuell, C. Zhao, T. Zobrist, "Alignment and use of the optical test for the 8.4m off-axis primary mirrors of the Giant Magellan Telescope," Proc. SPIE **7739**, (2010).

[5] T. L. Zobrist, J. H. Burge and H. M. Martin, "Accuracy of laser tracker measurements of the GMT 8.4 m off-axis mirror segments", Proc. SPIE **7739**, (2010).

[6] R. G. Allen, J. H. Burge, P. Su and H. M. Martin, "Scanning pentaprism test for the GMT 8.4 m off-axis segments", Proc. SPIE **7739** (2010).

[7] P. Su, R. E. Parks, L. Wang, R. P. Angel, and J. H. Burge, "Software configurable optical test system: a computerized reverse Hartmann test," Applied Optics **49**(23), pp.4404-4412 (2010).

[8] P. Su, Y. Wang, J. H. Burge, M. Idir, K. Kaznatcheev, "Non-null full field X-ray mirror metrology using SCOTS: A reflection deflectometry approach," Opt. Exp. **20**, 12393-12407. (2012)

[9] T. Bothe, W. Li, C. von Kopylow, and W. Jueptner, "High resolution 3D shape measurement on specular surfaces by fringe reflection," Proc. SPIE **5457**, 411–422 (2004).

[10] M. Knauer, J. Kaminski, and G. Hausler, "Phase measuring deflectometry: a new approach to measure specular free form surfaces," Proc. SPIE **5457**, 366–376 (2004).

[11] M. Sandner, W. Li, T. Bothe, J. Burke, C. v. Kopylow, and R. B. Bergmann, "Absolut-Abstandsreferenz für die Streifenreflexionstechnik zur Verringerung systematischer Messfehler," in Proceedings of DGaO 2011 (2011).

[12] D. Malacara-Doblado and I. Ghozeil, "Hartmann, Hartmann-Shack, and other screen tests," in Optical Shop Testing, 3rd ed., D. Malacara, ed., (Wiley, 2007) pp. 361–397.

[13] J. H. Burge, P. Su, C. Zhao, and T. Zobrist, "Use of a commercial laser tracker for optical alignment," Proc. SPIE **6676**, (2007).

[14] J. L. Rayces, "Exact relation between wave aberration and ray aberration," Optica Acta: International Journal of Optics **11**(2), 85-88 (1964).

[15] C. Zhao and J. H. Burge, "Orthonormal vector polynomials in a unit circle, Part I: basis set derived from gradients of Zernike polynomials," Optics Express **15**(26), 18014-18024 (2007).

[16] C. Zhao and J. H. Burge, "Orthonormal vector polynomials in a unit circle, Part II: completing the basis set," Optics Express **16**(9) 6586-6591 (2008).